THE ASTROPHYSICAL JOURNAL, 237:438–449, 1980 April 15

ROCKET-ULTRAVIOLET IMAGERY OF THE NORTH AMERICA NEBULA

GEORGE R. CARRUTHERS,[1] HARRY M. HECKATHORN,[1] AND THEODORE R. GULL[2]
Received 1979 August 7; accepted 1979 October 18

ABSTRACT

Ultraviolet imagery, in the wavelength range 1230–2000 Å with about 40″ resolution, has been obtained of the North America Nebula (NGC 7000) and surrounding regions with an electrographic Schmidt camera in a sounding-rocket flight. Visual imagery of this region was obtained with narrow-passband interference filters individually isolating several nebular emission lines and blue continuum. NGC 7000 was also observed in the far-UV with a nebular spectrograph in a sounding rocket flight.

The integrated brightness of NGC 7000 near 1450 Å is unexpectedly high (3 ± 1 times the directly observed brightness of the star HD 199579), yet no emission lines were observed with the nebular spectrograph. Hence, it is concluded that the recorded UV image is due to dust scattering of stellar continuum. Although the UV image is unlike the nebular emission line images, a quantitative comparison with the blue continuum image is not possible because of dominant contributions to the latter by hydrogen recombination continuum, night sky background, and unresolved faint stars.

It is shown that the high UV brightness of NGC 7000 can be accounted for by the scattered continuum radiation of other O stars, in addition to HD 199579, also located within the H II region, and/or a large optical depth for dust scattering by grains with very high albedo, resulting in relatively little net loss of scattered photons.

Subject headings: nebulae: general — nebulae: individual — ultraviolet: spectra

I. INTRODUCTION

The North America Nebula (NGC 7000) is one of the larger (in angular size) and more studied galactic H II regions. Its surface brightness is substantially lower than that of the Orion Nebula, and therefore it has not been investigated as thoroughly. However, NGC 7000 has been the subject of several photometric studies in various nebular emission lines (see Pottasch 1965 for a review; also Krishna Swamy and O'Dell 1967; Ishida and Kawajiri 1968; Goudis and Meaburn 1973; Goudis and Johnson 1978). Recently, Parker, Gull, and Kirshner (1979) have surveyed the Milky Way by direct imagery through narrow-band interference filters centered on several nebular emission lines and continuum. This survey includes fields covering the North America Nebula.

In the ultraviolet wavelength range below the ground-based limit of 3000 Å, observations of NGC 7000, and of galactic H II regions in general, are scarce. The only previous UV imagery of NGC 7000 is that obtained with the S201 Far-Ultraviolet Camera on the *Apollo 16* mission (Carruthers and Page 1976) which covered the 1250–1600 Å range. To our knowledge there exist no previous far-ultraviolet spectra of this object. Until the *International Ultraviolet Explorer* (*IUE*) was launched, the only far-UV spectrum of a galactic H II region was that of the Orion Nebula obtained by Bohlin and Stecher (1975). However, there have been numerous observations of planetary nebulae and the Cygnus Loop supernova remnant by sounding rockets, by *IUE*, and by the ultraviolet spectrometers on the two *Voyager* spacecraft.

In this paper, we report new ultraviolet imagery of NGC 7000 obtained in a sounding-rocket flight with an electrographic Schmidt camera which covers the 1230–2000 Å wavelength range and which has higher angular resolution than the *Apollo 16* imagery. We also compare the UV imagery with ground-based imagery—in particular, that obtained by Parker, Gull, and Kirshner. "Quick look" results of a far-ultraviolet nebular spectrograph rocket flight in which NGC 7000 was observed are presented, and implications of all of the above regarding the source of the observed ultraviolet brightness distribution are discussed.

II. OBSERVATIONS

a) Far-UV Imagery

The electrographic camera and the observing program used for the NGC 7000 direct imagery have been previously described by Carruthers, Heckathorn, and Opal (1978) (herein called Paper 1). The North America Nebula was observed with exposure times of 4.3, 50.9, and 9.7 s in the latter portion of a sounding-rocket flight (NASA 26.056 DG, launched 1976 October 29) whose primary objective was imagery of the Andromeda Galaxy, M31. The objectives of the NGC 7000 observations were (*a*) to obtain improved-resolution imagery of this object, and (*b*) to observe a star field overlapping one of the fields observed by the

[1] E. O. Hulburt Center for Space Research, Naval Research Laboratory.

[2] Laboratory for Astronomy and Solar Physics, Goddard Space Flight Center.

S201 instrument, so that the camera calibrations could be compared through analysis of images of stars recorded by both instruments.

As mentioned in Paper 1, coronal discharge occurred within the instrument during the flight, which produced background fogging of localized areas of the images. In the latter portion of the flight, during which NGC 7000 was observed, this discharge fogging was far less severe than when M31 was observed. Therefore, this fogging produced little or no adverse effect on the areas of the frames which contained NGC 7000.

Figure 1 (Plate 23) shows a portion of the far-UV image (50.9 s exposure) including NGC 7000 and the 68 Cygni H II region, and, for comparison, the Palomar Sky Survey blue print of this area. The diffuse nebulosity correlates very well between the two images; even the boundaries of the dark cloud separating the two H II regions is evident in both images. However, there are some subtle differences.

Since both the blue and far-UV images cover relatively wide wavelength ranges, it is not possible to determine from this comparison whether the far-UV image is due to emission lines or to dust scattering of hot-star continuum. Such a determination is aided by comparing the UV image with ground-based images in specific emission lines and in line-free regions of continuum.

b) Ground-based Narrow-Band Imagery

Figure 2 (Plate 24) is a comparison of the far-UV image with several images of NGC 7000 as recorded in the emission-line survey by Parker, Gull, and Kirshner. These latter images include the blue continuum (4215 Å, $\Delta\lambda = 40$ Å), and emission lines ranging from low-excitation [S II] to higher-excitation [O III]. The [S II] image was recorded through a 40 Å bandpass at 6725 Å. As noted by Gull (1974), Lada *et al.* (1976), and Balick, Gull, and Smith (1980), this emission has its greatest emission measure in H II regions near the ionization boundaries of dark clouds; hence "bright rims" are prominent in this bandpass. The Hβ (4861 Å, $\Delta\lambda = 28$ Å) and Hα + [N II] (6570 Å, $\Delta\lambda = 70$ Å) imagery shows a diffuse, nearly uniform structure within the nebula with few prominent bright rims. Finally, the [O III] emission (28 Å bandpass at 5007 Å) is characteristic of higher-excitation ionized gas (such as is found near stars with spectral types earlier than O9.5 or in shocked regions). In NGC 7000 [O III] seems concentrated toward the interior of the nebula and does not show bright rim features.

In comparing the UV image with the 4215 Å continuum image, it is apparent that the far-UV reveals far fewer stars. Most stars are too cool to emit a sizable fraction of their radiation at wavelengths shortward of 2000 Å; only those stars which are sufficiently hot (those of spectral types O and B) and which are not heavily reddened by interstellar dust, appear much brighter in the UV than they do in the visible (see Fig. 10).

Figure 3 (Plate 25). shows enlargements of the NGC 7000 UV image. Dust lanes and dark dust clouds which project in front of the nebula are much more apparent in the UV image than in ground-based imagery, probably because of the much higher extinction coefficient of interstellar dust in the far UV compared to the visual range. Most strikingly apparent in Figure 3 is a prominent dark cloud just to the northeast of HD 199579 (SAO 050263), which is only marginally detectable on the visible photographs, as is a dark lane further to the north and east. On the other hand, the apparent dark lane southeast of HD 199579 (which passes through "Texas" of the North America Nebula) shows less contrast in the UV than in the visible emission lines; perhaps this is a region of low ionization density rather than of foreground extinction.

c) Far-UV Spectra

The North America Nebula was observed with a new far-UV nebular spectrograph in a sounding-rocket flight (NASA 25.027 DG) launched 1979 June 2. The instrument, which is described by Carruthers (1979), was equipped with an entrance slit subtending an angular area of 2′ by 2°.8, and was capable of angular resolution along the slit of about 3′. During the flight, the only emission line feature recorded was the Lα (1216 Å) geocoronal line. Fortuitously, the star HD 199579 was included in the spectrograph slit for some of the exposures, and its spectrum was recorded on those frames. Preliminary estimates based on the observed brightnesses of the geocoronal Lα and of the HD 199579 spectra allowed us to place upper limits of about 10–20 rayleighs (R) (in the range of peak sensitivity, roughly 1200–1600 Å) on the intensities of any emission line features due to NGC 7000.

III. DATA ANALYSIS

The 50.9 s exposure far-UV image was scanned on the Grant microdensitometer at NRL, in the same manner as was the M31 imagery (Paper I). The recorded densities were corrected for the nonlinear response of the Kodak NTB-3 recording emulsion as previously, but the densities in the nebular region (less than $\sim$0.7 density unit) are in the range where the density-exposure relationship is essentially linear. Isodensity contour plots were generated by computer processing of the tape-recorded microdensitometry. Figure 4 shows a contour plot at intervals of 0.04 density unit above sky background, and Figure 5 shows a plot of the inner regions of the nebula at intervals of 0.02 density unit.

The diffuse source sensitivity of the camera was determined, using the preflight calibration discussed in Paper I, to be 0.0058 density unit $kR^{-1}\,s^{-1}$ at 1304 Å. This measurement was combined with the separately measured spectral response curve of the camera to yield the diffuse source sensitivity versus wavelength, shown in Figure 6. For comparison, the corresponding preflight calibration of the S201 instrument (Carruthers and Page 1976) is also plotted. The response curves shown reflect the differences in focal ratio and accelerating voltage, as well as overall

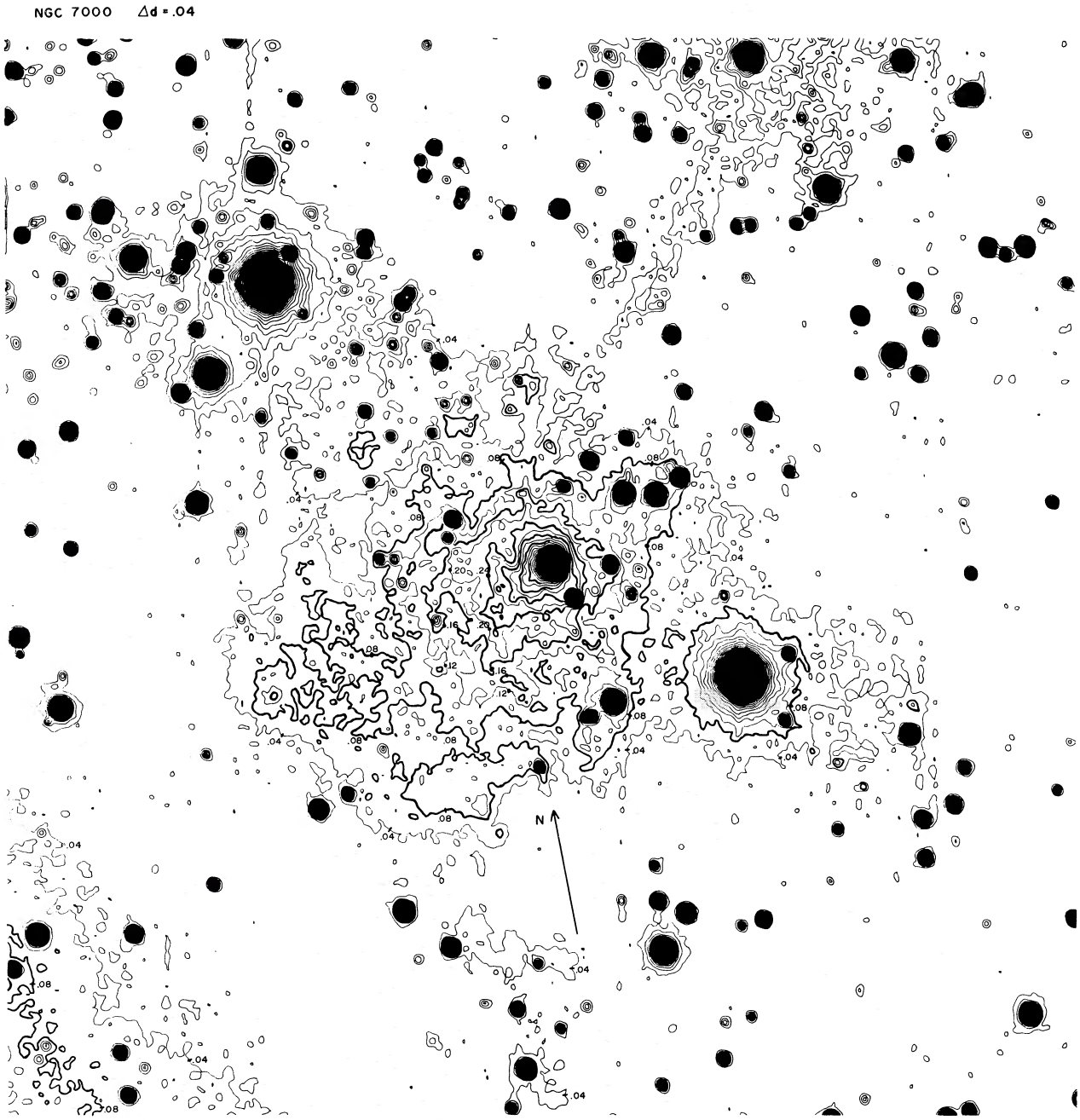

FIG. 4.—Isophotal contour map of the North America Nebula generated from microdensitometry of the far-UV image. The digitized data were lightly smoothed and corrected for (small) photometric nonlinearities as described in Paper I. The faintest isophote (labeled 0.04) is 7% above sky background, and the interval between successive contours is 0.04 density.

quantum efficiency versus wavelength, between the two instruments.

If we assume that the emission from NGC 7000 is concentrated in an emission line at the effective wavelength (1450 Å) of the camera response curve, the diffuse source sensitivity of the camera for the 50.9 s exposure time is found to be 0.23 density unit per kR, or 0.02 density unit = 88 R. If we assume the emission is a flat continuum (photon flux independent of wavelength), over the 450 Å effective passband of the camera, this corresponds to 0.02 density unit = 0.196 R/Å.

We note from Figures 4 and 5 that quite high brightness levels were recorded in the vicinity of the star HD 199579. This rise is not totally due to instrumental scattering of light from HD 199579 as is demonstrated by the marked asymmetry of the contour levels; there is a relatively low nebular brightness

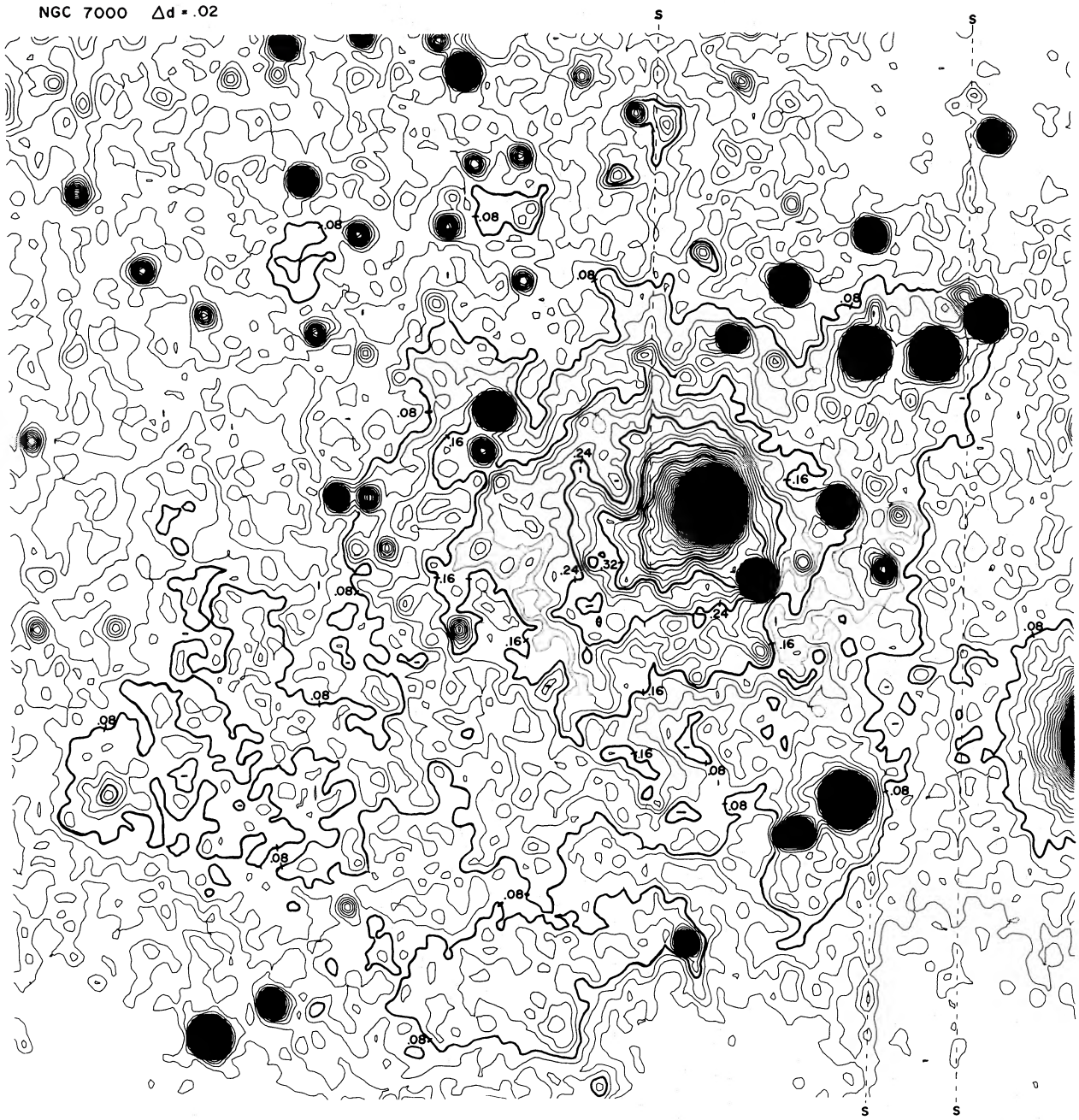

FIG. 5.—Far-UV isophotal contour map of the inner region of the North America Nebula generated in the same manner as Fig. 4. The contour interval is 0.02 density.

just to the west of the star image which is probably due to dust extinction. For comparison, the much brighter stars 57 Cyg and 60 Cyg show a uniform decrease in all directions, and the apparent structure is probably due to instrumental scattering. As a qualitative check on the instrumental star-image "blooming" contribution to the apparent nebular brightness levels near the stellar image, we compared the image profile of HD 199579 plus the surrounding nebulosity with image profiles of other stars, which are outside the nebula and are of comparable brightness to HD 199579. We also compared the mean image profiles on opposite sides of the HD 199579 image, where (as noted) there appeared to be marked asymmetry in the nebular brightness contours. (See Paper I, § III*b*, for the method used to determine these image profiles.)

Figure 7 compares the image profiles of HD 199579 and surrounding nebulosity, from the northwest (low nebular brightness) and from the southeast (high nebular brightness) directions. The difference between these distributions, also plotted in Figure 7, is a measure of the true nebular brightness difference and

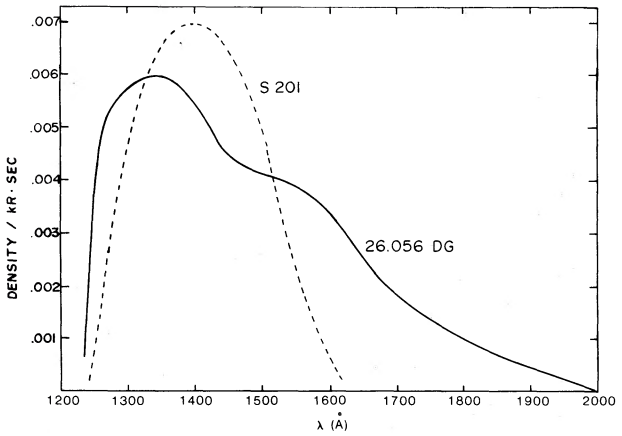

FIG. 6.—The sensitivities of two electrographic Schmidt cameras to a diffuse source (specified as optical density on the recording emulsion per kilorayleigh second) as a function of wavelength. The NGC 7000 imagery discussed here was obtained during NASA sounding rocket flight 26.056 DG while somewhat lower resolution imagery was conducted by the S201 camera on the *Apollo 16* mission. The curves shown are based on preflight calibration measurements.

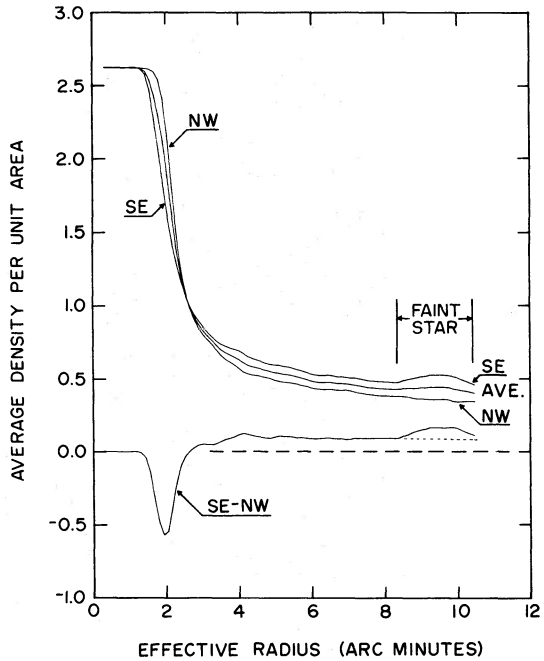

FIG. 7.—The mean UV brightness profile (labeled AVE.) for HD 199579. The quantity plotted on the ordinate is the average optical density per unit area on the emulsion at the effective radius of an annular region of thickness ~ 7″ centered on the position of HD 199579. It includes contributions from the star, nebula, and sky background. At densities greater than about 2.5, the microdensitometer becomes saturated—resulting in the "flattopped" profile. The curves labeled SE and NW represent the brightness profiles computed in "half-annular" regions centered on HD 199579 and extending toward the direction of high and low nebular brightness, respectively. The difference between these latter curves (labeled SE − NW) reveals some assymetry in the image of the star interior to ~ 3′ radius (caused by the camera optics), but is a measure of the true nebular brightness difference at greater radii and therefore should be independent of instrumental scattering of starlight.

should be independent of instrumental scattering of starlight.

Figure 8 compares an image profile near HD 199579, with the average of similar profiles for three stars judged comparable in brightness to HD 199579. The individual stellar profiles showed quite good agreement with each other, which indicates that the shape and extent of the profile is not a sensitive function of the star brightness for such vastly overexposed images. Hence, subtraction of the averaged profile from that of HD199579 should give a good indication of the net nebular brightness except for the region in the star image where microdensitometer saturation becomes important or where the profiles are particularly steep. As is seen from Figure 8, the nebular brightness shows only a modest and gradual increase in the near vicinity of the star. The brightness of the nebula (as represented by the "difference" profile in Fig. 8) is such that a mean density of ~0.35 (corrected for sky and instrumental backgrounds and for instrumental scattering) is reached at a distance of ~3′ on the SE side of HD 199579. This, therefore, corresponds to an emission intensity of 1540 R, or 3.4 R/Å at 1450 Å.

Quantitative comparisons of the UV imagery with the ground-based imagery of Figure 2 are difficult, since the latter images were not recorded with an immediate goal of doing quantitative photometry. However, a qualitative comparison of the brightness distributions can be done by comparing microdensitometer scans along selected strips of the UV image and the visible images after applying a crude calibration to the latter. As shown in Figure 3, this was done for a strip between SAO 050382 and SAO 050219, which also passes through the image of HD 199579, on each frame. Calibration wedge exposures, developed simultaneously with the ground-based imagery, were microdensitometered to provide the conversion from photographic density to intensity units. In the areas scanned in the visible imagery the exposure levels were such that all of the measured densities fell on the "linear portion" of the characteristic curve (i.e., at photographic densities greater than 0.5 above chemical fog). We measured a value of $\gamma = 2.9$ for the nitrogen baked IIIa-J photographic emulsion and assumed a linear relation between photographic density and log of intensity—a procedure which is more than adequate for our qualitative comparison. Relative intensities along the strip scans in the ground-based imagery are compared with that for the far-UV imagery in Figure 9. The intensity distributions have been plotted on a logarithmic scale to better intercompare their shapes. In the blue continuum and [S II] images, where the nebular brightness is low, the brightness distributions are confused by numerous faint star images. Indeed, the brightness levels within the nebula for these two images may be enhanced by unresolved stars.

IV. DISCUSSION

It is readily apparent, from inspection of Figure 9, that there are significant differences between images

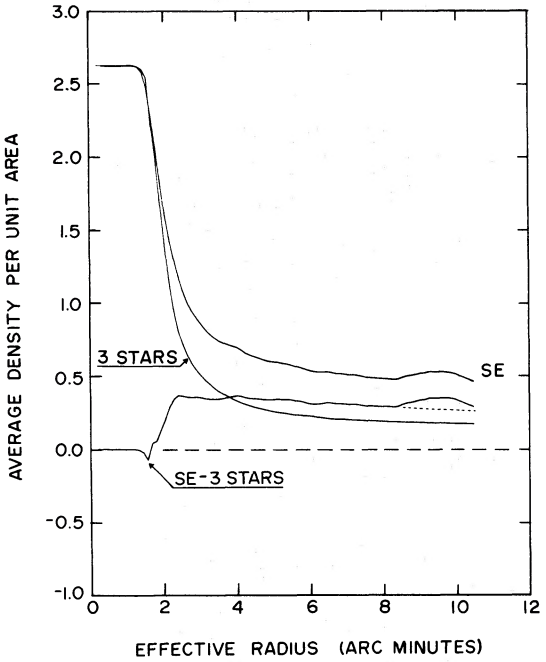

FIG. 8.—The UV brightness profile of HD 199579 (high nebular brightness side) with the average of similar profiles for three stars (SAO 049946, 050274, 050303) judged to be comparable in brightness by visual inspection of the far-UV imagery. The difference between the profiles gives an indication of the net nebular brightness except in the saturated region or where the profiles are particularly steep (i.e., at radii less than ~ 2'.5).

obtained in different wavelength ranges and in different emission lines. The [O III] and hydrogen emissions have similar brightness distributions in the inner regions of the nebula, but the [O III], blue continuum, and UV images do not show the "bright rim" features apparent in the lower-excitation [S II] image. The UV brightness distribution is unlike any of the visible distributions, in that it shows a steeper rise in brightness close to the O star HD 199579, but at the same time its faint structure appears to extend much further (particularly in the northeast direction, toward the bright B star 60 Cyg) than does the [O III] image. The blue continuum image has a very flat brightness distribution, with only a slight hint of an enhancement in the vicinity of HD 199579, but night sky background contributes most of the radiation recorded in this passband, and also faint star images may contribute to the nebular continuum level.

The increased nebular UV brightness near HD 199579, relative to that of the blue continuum or [O III] brightnesses, suggests that some of the radiation detected in the near vicinity of HD 199579 might be emitted by highly ionized elements which are photoionized within a Strömgren sphere that is much smaller than the H^+ or O^{++} ionization spheres. Osterbrock (1963) has discussed in detail the expected ultraviolet emission line spectra of gaseous nebulae. His paper predicts relative intensities of emission lines per unit abundance of a given ion; however, the abundance of a specific ion is determined by the elemental abundance and by photoionization equilibrium. The computed extreme-ultraviolet flux distributions of early type stars of Kurucz (1979) (see Fig. 10), and the photoionization thresholds of plausibly abundant species, predict that the likely far-UV emission lines in the 1230–2000 Å range would include those of Si IV near 1400 Å, C IV near 1550 Å, and C III] near 1909 Å. Our nebular spectrograph rocket flight, however, placed upper limits of 10–20 R on the intensities for the Si IV and C IV emissions in the brighter regions of NGC 7000. (Both the nebular spectrograph and the Schmidt camera used CsI photocathodes which had very low sensitivity to C III] λ1909.) Since integrated brightnesses exceeding 1 kR were measured in the direct imagery of NGC 7000, less than a few percent of the observed far-UV radiation is due to emission line radiation.

The ultraviolet spectra of the Orion Nebula obtained by Bohlin and Stecher (1975) revealed that, except for a weak C III] emission line at 1909 Å, the nebula exhibited only a continuous spectrum between 1250 and 2000 Å. (Such is confirmed by more recent observations of this nebula by *IUE* [C. Harvel, private communication].) Bohlin and Stecher interpret this continuum as due to scattering of the ultraviolet light of the embedded hot stars by dust. Indeed, the continuum has absorption lines at the wavelengths of known absorptions in the spectrum of θ Ori. Ground-based observations (O'Dell and Hubbard 1965; Schiffer and Mathis 1974; Dopita, Isobe, and Meaburn 1975) also demonstrate that the Orion Nebula has a visible-range continuum intensity well above the expected recombination continuum. The strength of the continuum increases (relative to hydrogen emissions) toward the outer parts of the Orion Nebula, and is indicative of dust scattering of starlight. Peimbert and Goldsmith (1972) detected the He II 4686 Å absorption line in the continuum of the Orion Nebula, further demonstrating the dust-scattering origin of the continuum.

However, Krishna Swamy and O'Dell (1967) found that for NGC 7000 there was little or no excess continuum above the expected atomic continuum, indicative of little dust-scattering contribution. Therefore, we would not have expected NGC 7000, like the Orion Nebula, to have a primarily continuous spectrum in the far-UV.

Unfortunately, our longest (67 s) spectrographic exposure is not quite adequate for accurate measurements of the continuous nebular spectrum at the level of integrated brightness measured by the direct imagery. However, the apparent absence of appreciable line emission is of great significance to interpretation of the direct imagery.

There is a discrepancy between the brightness of NGC 7000 reported here and that measured with the S201 instrument (Carruthers and Page 1976), as the presently measured nebular brightness is much higher. The observed image densities in the 10 minute S201 exposure and the 50.9 s rocket exposure were quite similar, yet Figure 6 shows that the diffuse source sensitivities indicated by preflight calibrations of the two cameras were comparable near 1450 Å. The 0.08

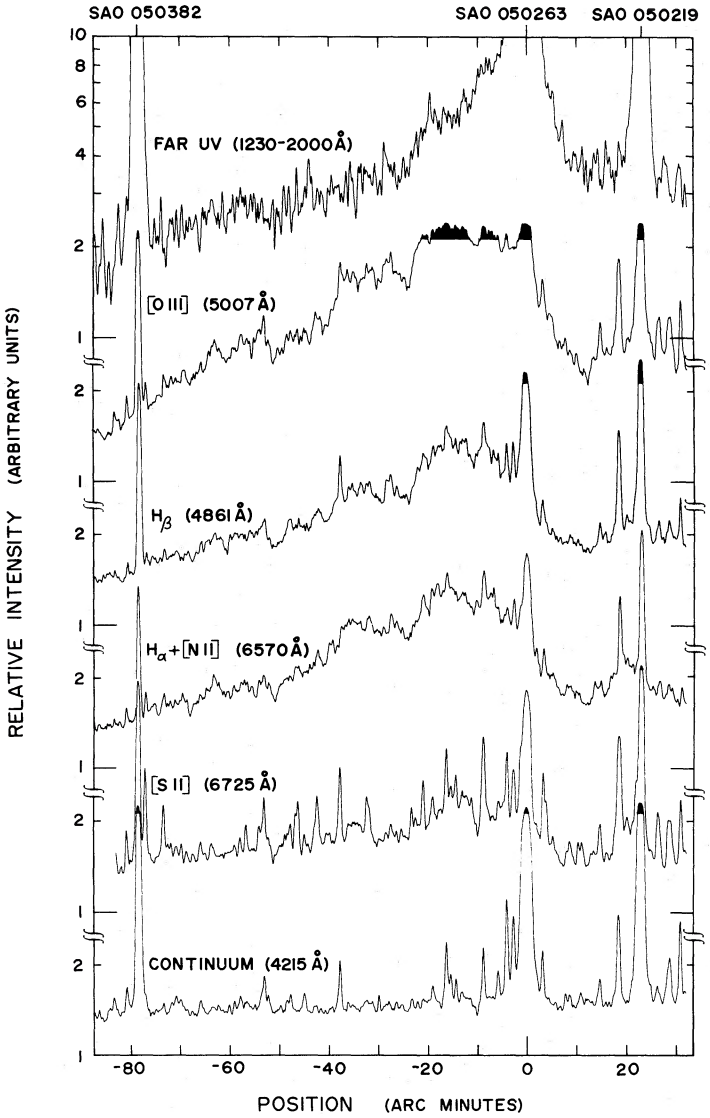

FIG. 9.—Comparison of the far-UV and visible brightness distributions measured from the imagery presented in Fig. 2. The comparison is made along a strip (see Fig. 3 for orientation) chosen to maximize the asymmetry of the far UV brightness distribution around HD 199579. The effects of microdensitometer saturation are indicated (see, e.g., the region extending from HD 199579 to ~20′ SE on the [O III] scan); here the plotted intensity should be considered a lower limit.

density (350 R) contour of Figures 4 and 5 corresponds closely to the 0.2 density (56 R) contour of Carruthers and Page (their Fig. 5), a factor of 6 discrepancy.

If the nebular emission were a flat continuum distribution, then the response curves in Figure 6 indicate that a factor of 2 difference in brightness would be accounted for as a result of the broader bandpass of the rocket instrument. However, this still leaves a factor of 2 to 3 discrepancy which would indicate that the absolute sensitivity of one or both instruments at the times the observations were made differed from that determined before flight.

Further investigation of the actual in-flight instrument sensitivities was made by detailed comparison of the images of stars viewed by both instruments. To this end, the overlapping portions of the S201 and rocket frames were examined for star images which could be suitably compared by microdensitometry of both sets of imagery on the Grant machine at NRL. The criteria were that the star image not be saturated on at least the 4.3 s exposure rocket frame, yet be readily measurable on one or both of the 3 minute and 10 minute exposures of the Cygnus region obtained with the S201 instrument in the 1250–1600 Å wavelength range; also, that the stars have reasonably accurate ground-based spectral classifications and photometry. We found only two stars satisfying these criteria: HD 202124 = SAO 050567 [O9.5 Ib, m_V = 7.80, $E(B-V) = 0.52$] and HD 199356 = SAO 050230 [B2 IV, $m_V = 7.16$, $E(B-V) = 0.40$] (Blanco *et al.* 1970). These stars were scanned on the 4.3 s rocket exposure and the 3 minute and 10 minute S201

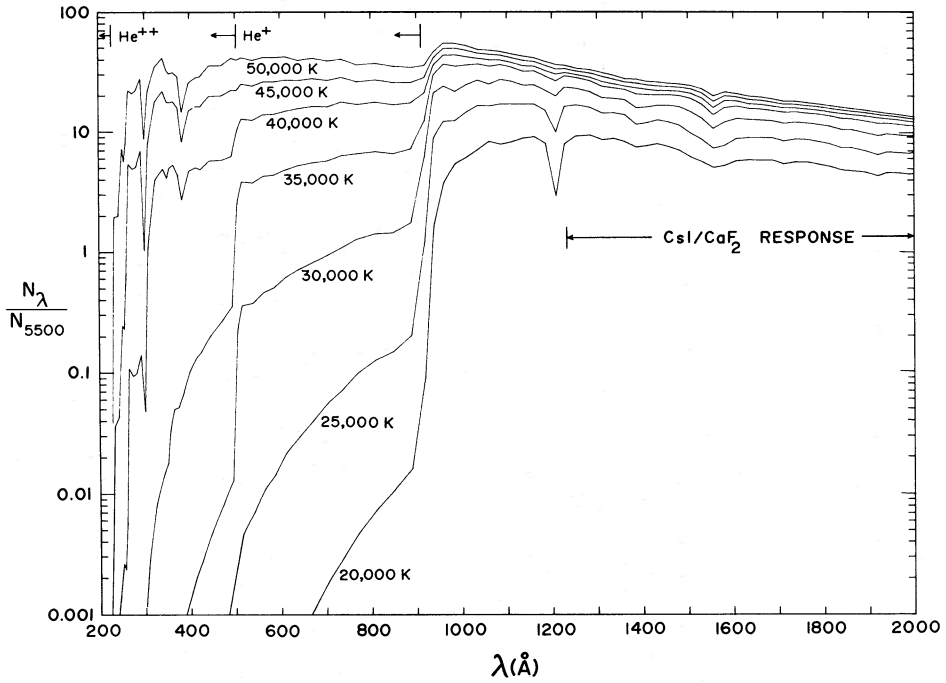

FIG. 10.—Theoretical ultraviolet flux distributions for main-sequence, unreddened early type stars as predicted by the line-blanketed model atmospheres calculated by Kurucz (1979). The theoretical photon flux (photons cm^{-2} s^{-1} $Å^{-1}$) normalized to 5500 Å is plotted as a function of wavelength for stars with solar abundances. The surface gravity for the four coolest models presented is log g = 4.0 and for the higher temperature models log g = 4.5. The ground state continuum for neutral hydrogen and helium and for singly ionized helium are indicated as is the region of sensitivity for the electrographic Schmidt camera.

exposures, their density volumes determined (see Paper 1), and the measurements compared with expectations based on folding of the instrument preflight calibrations with model atmosphere flux distributions and the Bless and Savage (1972) "average" extinction curve. For HD 202124, we found a factor of 100 higher sensitivity for the rocket instrument versus S201, whereas only a factor of 40 was expected. In the case of HD 199356, a factor of 66 was found; however, even the 4.3 s rocket exposure rocket image of this star was on the verge of saturation, and hence its brightness may have been underestimated.

An independent check on the S201 sensitivity is afforded by the fact that the image of HD 199579, for which photometric measurements by *OAO 2* at 1330 Å and 1430 Å exist (Code, Holm, and Bottemiller 1977, hereafter CHB), was unsaturated in 3.0 and 3.7 minute exposures as measured in the original scans with a PDS microdensitometer (Carruthers and Page 1976; Page, Carruthers, and Hill 1978). A computer printout of PDS density versus position, for each point of the scans near HD 199579, was used to obtain a density volume for the HD 199579 image on the 3 minute exposure. The appropriate nebular background level to be subtracted was estimated by comparing scans through the nebula on the 10 minute S201 exposure and the 50.9 s rocket exposure (see Fig. 11; the inward extrapolation to the center of the star image was obtained using Fig. 8). The derived density volume, converted to intensity as in Page, Carruthers, and Hill (1978) and to an ultraviolet magnitude as per CHB, yields m(1400 Å) = 3.68, in excellent agreement with m(1430 Å) = 3.66 obtained by CHB.

The stars HD 199356 and HD 202124 were not included in the measurements of CHB, but have been observed by the S2/68 instrument on the *TD 1* satellite (Thompson *et al.* 1978). For HD 199356, m(1565 Å) = 5.63, m(9965 Å) = 6.15; for HD 202124, m(1565 Å) = 7.16, m(1965 Å) = 7.33. When compared with expectations based on model atmosphere predictions and the "average" interstellar extinction curve of Bless and Savage (1972), the 1565 Å satellite measurements (particularly for HD 202124) fall below the expected flux. The nature of the deviation is such as to suggest a steeper-than-average interstellar extinction curve for this region, i.e., one having a "minimum" closer to 2000 Å than to the typical 1600 Å. The ratio of the brightnesses of the two stars as measured on the 3 minute S201 exposure is in good agreement with the trend of the *TD 1* observations. These indicate that, in fact, HD 202124 has an observed color in the 1230–2000 Å range about the same as an unreddened 9500 K model, for which we computed an expected sensitivity ratio for the two cameras of about 50.

We are, therefore, still faced with a factor of 1.5 to 2.0 higher-than-expected ratio of the rocket camera sensitivity to the S201 camera sensitivity. We indicated in Paper I that the brightness of the central region of M31 as measured with our rocket camera, based on the preflight calibration, was a factor of 1.5 higher than indicated by the measurement of Code and Welch (9979). Thus, the camera seems well established

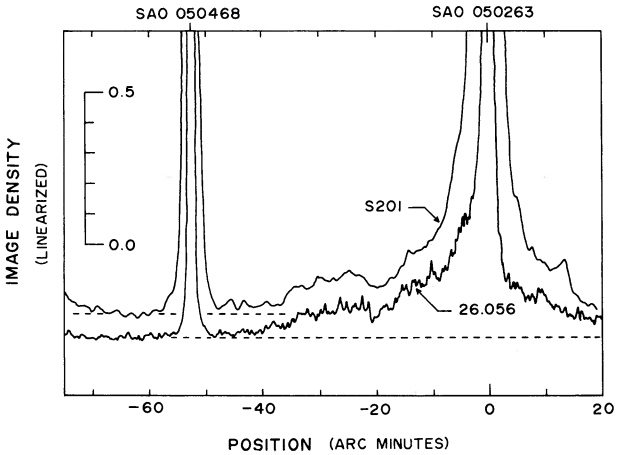

FIG. 11.—Comparison of far-UV brightness distributions measured from the 50.9 s exposure rocket image (NASA 26.056) and from the 10 minute exposure S201 imagery from *Apollo 16*. Both scans were made with a Grant microdensitometer along a strip passing through SAO 050468 and SAO 050263 (see Fig. 3 for orientation). The ordinate scale zero points for the two scans have been shifted to avoid overlap of the profiles, but the instrumental plus sky background levels have been indicated by dashed lines.

to have had an absolute sensitivity 1.5 times higher than was indicated by our preflight calibration. Unfortunately, we cannot directly compare the rocket camera sensitivity with any of the stars observed by CHB; even the 4.3 s exposure of HD 199579 is saturated.

A more detailed comparison of the nebular brightness distributions as measured by the two instruments can be made from scans of both films with the same microdensitometer and settings as for the star images; the results of a scan through the nebula along the path through SAO 050468 and HD 199579 is shown in Figure 11. It is seen that the structural details as revealed in the two different images agree quite well. The density levels in the S201 exposure are a factor of about 1.3 higher. However, since the exposure time was longer by a factor of 11.8, the density/exposure, or diffuse-source sensitivity, is a factor of 9 higher for the rocket instrument.

The diffuse-source sensitivity ratio for the two cameras is known as a function of the point-source sensitivity ratio, *assuming both the stars and the nebula have the same spectral distribution*, since only geometrical factors are involved. The preflight calibrations, as previously mentioned, indicated factors of 40–50 point-source ratio (for typical stellar flux distributions), whereas the star image comparison indicated factors of 70–100 (the *TD 1* observations indicate very similar far-UV colors for HD 199579 and one of our comparison stars, HD 199356). The preflight calibrations predict a 2.4–3.0 broad-band diffuse-source sensitivity ratio in favor of the rocket camera, whereas the star-image comparison indicates a ratio of 4.5–6.0. Thus, even after correcting for the observed point-source sensitivity ratio, there is still a factor of 1.5 higher nebular brightness in the rocket image still to be accounted for. Therefore, it appears that the *spectral distribution of the nebular radiation* must be peculiar in such a way as to further favor the rocket instrument, i.e., by being exceptionally high at short (below 1300 Å) or long (above 1500 Å) wavelengths, where the S201 instrument is relatively less sensitive than in the intermediate (1400 Å) range (see Fig. 6).

The integrated ultraviolet brightness of NGC 7000 can be compared with that of the star HD199579 as done previously for ultraviolet imagery of the Orion Nebula (Carruthers and Opal 1977*b*). Such a comparison is of limited use in quantitative interpretation of the nebular radiation, because the extinction over the face of the nebula is large and quite variable, plus there are great uncertainties regarding internal reddening effects and nebular geometry. However, such a comparison is qualitatively useful and enlightening.

A lower limit of integrated brightness, which should be within 20% of the actual value, was obtained using a planimeter to integrate the contour plot of Figure 4. If the radiation is assumed to be a flat continuum, and using the preflight calibration of the camera sensitivity (0.02 density = 0.196 R/Å), the integrated brightness is found to be 42 photons cm^{-2} s^{-1} $Å^{-1}$. If we lower this by a factor of 1.5 to account for the indicated higher-than-expected camera sensitivity, this becomes 28 photons cm^{-2} s^{-1} $Å^{-1}$. However, the 1430 Å brightness of the star HD 199579 reported by CHB corresponds to only 9.67 photons cm^{-2} s^{-1} $Å^{-1}$, and their 1330 Å brightness to 8.29 photons cm^{-2} s^{-1} $Å^{-1}$. Thus, the nebula appears to be 3 times as bright as the star in the wavelength range covered; taking into account the uncertainties of the camera calibration and measurement errors gives this ratio with plausible range of uncertainty to be 3 ± 1.

If we take into account the effect of interstellar extinction on the observed UV flux from HD 199579, using the color excess $E(B - V) = 0.37$(CHB) and the "average" interstellar extinction curve of Bless and Savage (1972), giving $E(1430 - V) = 4.75 \times E(B - V)$, we find [assuming $A_V = 3.1E(B - V)$] a total extinction at 1430 Å of 2.9 mag, or a factor of 14.6. However, the extinction of the nebular radiation itself is certainly not negligible. In fact, Goudis and Johnson (1978) have shown that it is comparable to or greater than that for HD 199579. From their extinction map (obtained by comparing Hα measurements with radio continuum measurements of Felli and Churchwell (1972)), we estimate an average $A_V = 1.25$ [A(1430 Å) = 3.17] over the observable portion of the nebula. In the total absence of foreground dust lanes, such as the "Gulf of Mexico" and the dark lane separating the North America and Pelican nebulae, the total nebular radiation might be another factor of 2 greater than that deduced by correcting only the observed region for extinction.

Hence, even after correcting both the direct stellar radiation and the nebular radiation for foreground extinction, the integrated nebular brightness is considerably greater than the intrinsic stellar flux in the 1230–2000 Å range. This conclusion is not appreciably affected by the precise *shape* of the interstellar extinc-

tion curve, a matter which we will discuss later. There is extreme difficulty in accounting for so much nebular radiation by any mechanism, be it dust scattering of stellar continuum, or nebular emission lines. This may be seen from Figure 10, where it is shown that even for the hottest O stars the radiation flux shortward of 1230 Å is only comparable to that in the 1230–2000 Å range. Hence, even if there were a mechanism for total conversion of Lyman-continuum flux into far-UV continuum, it could not account for the observed far-UV nebular brightness.

Therefore, we consider our observations to be additional evidence for either (*a*) the presence of additional exciting stars besides HD 199579, hidden from view by the dense foreground dust clouds, and/or (*b*) a very low-loss scattering process for stellar UV continuum radiation to escape the H II region.

The presence of additional exciting stars in the NGC 7000–IC 5067 complex has also been indicated by the Hα and [N II] observations of Goudis and Meaburn (1973) and the radio continuum map of Felli and Churchwell (1972); see also Goudis and Johnson (1978). These indicate that the combined H II region is centered well south of the star HD 199579, and that the additional O star(s) is quite likely hidden by the dust lane which defines the "Gulf of Mexico." In principle, the total Lyman-continuum flux required to ionize an H II region can be derived from measurements of the total brightness of the H II region in Hα (if the extinction correction can be accurately determined) or in radio continuum (free-free emission). Morton (1969) has done this computation for several galactic H II regions, including NGC 7000. Assuming that HD 199579 is the only exciting star, he finds an effective temperature of about 53,000 K, well above that of a normal O6 star (about 40,000 K). Thus, the observed ionization requires at least one additional star of type O5 or earlier, or two or three additional O6 stars (see also Spitzer 1978, p. 110).

It we assume that the nebular radiation we observe is singly scattered stellar radiation, its integrated brightness cannot exceed the brightness of the illuminating stars. If the average extinction over the nebula is the same as that over HD 199579, our measurement would require at least 3 times the 1230–2000 Å flux of HD 199579, even if the dust were perfectly scattering and there were no extinction between the star(s) and the scattering dust.

Far-UV observations of dust reflection nebulae have indicated that interstellar dust grains exhibit high albedos in this wavelength range, and that the scattering phase function ranges from strongly forward-scattering in the visible and near-UV to more isotropic in the far-UV (Lillie and Witt 1973, 1976; Andriesse, Piersma, and Witt 1977; Witt 1977). Far-UV imagery and photometry of the Barnard Loop and the Orion Nebula (Carruthers and Opal 1977*a*,*b*; Witt and Lillie 1978) also support this finding. Thus, we may consider the possibility that, although both HD 199539 and the visible nebular radiation suffer about the same degree of extinction, the scattering by dust particles occurs with little net loss, and that therefore a much larger fraction of the stellar ultraviolet radiation escapes the nebula than would be the case if the extinction were due to pure absorption. Hence, although the attenuation of direct starlight is independent of the mechanism (whether it is scattering or pure absorption), this is not necessarily true for the nebular radiation.

The extinction toward HD 199579 at 1430 Å of 2.9 mag (assuming an "average" extinction curve) corresponds to an optical depth $\tau = 2.68$. If all the extinction is presumed to occur in or near the visible nebulosity, an optical depth this large implies that the ultraviolet photons observed from the nebulosity are multiply scattered. Hence, photons which would have been lost from view in an optically thin (singly scattering) medium may be scattered back into the line of sight. For perfectly scattering grains, in the optically thick limit, the total observed brightness of the nebula would equal the intrinsic luminosity of the star at any given wavelength, whereas the star itself would not be directly visible. If we assume an albedo of 0.6, which is indicated by previous measurements, and if we assume that each photon observed from the nebula has been scattered three times, the escape probability would be 0.216, which is 3 times the escape probability of photons coming directly to the observer from the star (0.069) and, in fact, accounts for the observed nebular/stellar brightness ratio of about 3. This would greatly reduce the requirement for flux from additional hot stars.

However, if at least the first scattering of UV photons is from dust within the H II region, and if this dust is similar to that in the Orion Nebula, it would have an appreciably different extinction curve from that applicable in the general interstellar medium (Bless and Savage 1972). To investigate this question further, an extinction curve for HD 199579 was derived by comparison of photometry by CHB (at 1330 Å) and *Copernicus* U2 spectra in the range 1000–1350 Å of Snow and Jenkins (1977) (SJ), for this star and for the lightly reddened O7 star 15 Mon. We find, from comparison of the CHB measurements, $E(1330 - V)/E(B - V) = 7.33$—a value well above even that for ζ Oph given by Bless and Savage (1972), and quite the opposite situation to that existing in the Orion Nebula region. Use of the U2 spectra for extrapolation to shorter wavelengths (and taking into account the change in U2 spectral response between the observations of the two stars, as given by Fig. 1 of SJ) reveals a curve which is slightly less steep than that for ζ Oph, reaching a value of $E(1100 - V)/E(B - V) = 11.1$ mag. An independent check on the extinction at 1330 Å can be made by assuming the intrinsic flux distribution of HD 199579 to be given by the 40,000 K model of Kurucz (1979) (see Fig. 10), and assuming $A_V = 1.15$ mag. This yields $E(1330 - V)/E(B - V) = 7.89$, in excellent agreement with the value of 7.73 obtained by reference to 15 Mon. As mentioned previously, the star HD 202124 and, to a lesser extent, HD 199356, also show high far-UV extinction.

Also of interest is that the U2 spectrum of HD 199579 shows strong absorptions due to interstellar H_2, whereas that of θ Ori does not, although its $E(B - V)$ of 0.32 (CHB; SJ) is comparable. These

results would appear to indicate that nearly all of the extinction (and dust scattering) is occurring in cold clouds well outside the H II region; however, the extent of this scattering region is limited by the observed angular size of the nebula in the UV image to, at most, a relatively thin shell surrounding the visible H II region. If the rise in extinction curves below 1600 Å is due to highly efficient scatterers (as opposed to absorbers, which probably produce the "2200 Å bump"), the fact that we find an unusually steep far-UV extinction curve toward HD 199579 lends further credence to the likelihood that scattering of far-UV starlight by dust particles occurs with unusually high efficiency in the NGC 7000 region.

As mentioned previously, Krishna Swamy and O'Dell (1967) found little or no visible continuum from NGC 7000 beyond the expected atomic continuum. Since this latter is due to hydrogen recombination, its spatial distribution should resemble that of Hα and Hβ, except for minor modifications by differential extinction. Therefore, since the dust scattering component of the visual continuum is a minor component, and (as mentioned previously) our present blue-continuum imagery is compromised by night sky and faint star contributions, it is not possible, with the data presently available, to meaningfully compare the scattering properties of dust in the visible and ultraviolet in this object. However, it may be possible in the future (by means of visible-continuum imagery of high photometric accuracy, with a subtractive technique referenced to comparable Hα or Hβ imagery to remove the recombination continuum contribution) to obtain more useful estimates of the visible dust scattering.

It is apparent that a detailed analysis of the radiative transfer by dust scattering in the nebula would be very useful, but uncertainties regarding the detailed scattering geometry, dust distribution within the nebula, and precise values of the albedo and scattering phase functions make such an analysis extremely challenging.

V. CONCLUSIONS AND RECOMMENDATIONS

Rocket-UV imagery of NGC 7000 implies an unexpectedly high brightness for this object near the star HD 199579. The emission intensity reaches a level as high as 2.3 R/Å at 1450 Å (adjusted by an indicated factor of 1.5 higher absolute sensitivity achieved in flight versus that deduced from the preflight calibrations). The integrated nebular brightness is at least 28 photons cm^{-2} s^{-1} $Å^{-1}$ at this wavelength, 3 times the brightness of HD 199579 as measured by CHB. An observation of NGC 7000 with a rocket nebular spectrograph revealed no nebular emission lines in excess of 20 R in the 1200–1600 Å range; hence, we conclude that the radiation observed in the UV image is nearly pure continuum.

Comparison of the UV imagery with ground-based narrow-band imagery in various nebular emission lines and blue continuum shows the UV brightness distribution to be unlike any of the nebular line brightness distributions. However, comparison with the blue continuum image is complicated by the fact that the latter image has dominant contributions due to night sky background, hydrogen recombination continuum (based on the work of Krishna Swamy and O'Dell 1967), and possibly unresolved faint stars. If the far-UV image is due to dust scattering of stellar continuum, then further quantitative understanding would require determination of its spectral distribution versus that of the star(s) and as a function of position in the nebula. A determination of the dust-scattering contribution to the visible continuum would also be useful; this in turn will require new blue continuum observations of very high photometric accuracy, using a subtractive technique to remove the night sky contribution, and (by reference to similar Hα or Hβ imagery) the recombination continuum contribution.

The absolute intensity of the UV image is a factor of 6 higher than that reported by Carruthers and Page (1976), a discrepancy which can partly be accounted for by differences in spectral responses of the two cameras used, partly by an inferred factor of 1.5 higher sensitivity for the rocket camera than expected from preflight calibrations (from comparisons of images of stars recorded in common by both instruments), and (possibly) by a nebular spectral distribution which rises sharply toward longer or shorter wavelengths within the 1230–2000 Å range (so as to favor the rocket instrument).

The present observations require one or both of the following, if the observed continuum is due to dust scattering of stellar radiation: (*a*) there are one or more additional O stars, having far-UV brightness(es) at least as large as that of HD 199579, in the NGC 7000 region but hidden from view by foreground dust clouds (a conclusion also inferred by other, previous observations); (*b*) the scattering dust is optically thick, but the scattering is highly efficient (high albedo) so that there is relatively little net loss of the scattered UV photons. Further credence to this latter suggestion is given by the fact that we find an unusually steep far-UV extinction curve in the direction of HD 199579, indicative of a large proportion of efficient scatterers in the dust in this region. With reasonable assumptions (average of three scatterings with albedo 0.6) it is possible to account for the observed nebular/stellar brightness ratio. However, a much more extensive modeling effort should be attempted for this object.

We thank NASA for its support of the sounding-rocket investigations and the ground-based survey, and Drs. Chet Opal, Robert Parker, and Thornton Page for their assistance and for useful discussions. We also thank D. King, H. Merchant, and many others for their support of the rocket experiment preparations and field operations.

Note added in manuscript 1979 December 12.— Further comparisons of stellar ultraviolet brightnesses as measured with the S201 instrument with those of *OAO 2* by CHB indicate that, although there is good

agreement in the case of HD 199579, for other stars in common the S201 measurements fall a factor of 2 or more below the *OAO 2* measurements. If the S201 sensitivity was, in fact, this amount lower than indicated by the preflight calibrations, this would further strengthen the case for a high UV brightness of NGC 7000 as indicated by the rocket observations discussed here.

REFERENCES

Andriesse, C. D., Piersma, T. R., and Witt, A. N. 1977, *Astr. Ap.*, **54**, 841.
Balick, B., Gull, T. R., and Smith, M. G. 1980, in preparation.
Blanco, V. M., Demers, S., Douglass, G. G., and FitzGerald, M.P. 1970, *Pub. US Naval Obs.*, Ser. 2, Vol. **21**(B).
Bless, R. C., and Savage, B. D. 1972, *Ap. J.*, **171**, 293.
Bohlin, R. C., and Stecher, T. P. 1975, *Bull. AAS*, **7**, 547.
Carruthers, G. R. 1979, in *Instrumentation in Astronomy–III* (Vol. **172** of Proceedings, Society of Photo-Optical Instrumentation Engineers), ed. D. Crawford, p. 304.
Carruthers, G. R., Heckathorn, H. M., and Opal, C. B. 1978, *Ap. J.*, **225**, 346 (Paper I).
Carruthers, G. R., and Opal, C. B. 1977a, *Ap. J. (Letters)*, **212**, L27.
———. 1977*b*, *Ap. J.*, **217**, 95.
Carruthers, G. R., and Page, T. 1976, *Ap. J.*, **205**, 397.
Code, A. D., Holm, A. V., and Bottemiller, R. L. 1977, Wisconsin Astrophysics, No. 31 (CHB).
Code, A. D., and Welch, G. A. 1979, *Ap. J.*, **228**, 95.
Dopita, M. A., Isobe, S., and Meaburn, J. 1975, *Ap. Space Sci.*, **34**, 91.
Felli, M., and Churchwell, E. 1972, *Astro. Ap. Suppl.*, **5**, 369.
Goudis, C., and Johnson, P. G. 1978, *Astr. Ap.*, **63**, 259.
Goudis, C., and Meaburn, J. 1973, *Astr. Ap.*, **26**, 65.
Gull, T. R. 1974, in H II *Regions and the Galactic Centre*, Proc. Eighth ESLAB Symposium, ed. A. F. Moorwood (ESRO SP-105), p. 1.
Ishida, K., and Kawajiri, N. 1968, *Pub. Astr. Soc. Japan*, **20**, 95.
Krishna Swamy, K. S., and O'Dell, C. R. 1967, *Ap. J.*, **147**, 529.
Kurucz, R. L. 1979, *Ap. J. Suppl.*, **40**, 1.
Lada, C. J., Gull, T. R., Gottlieb, C. A., and Gottlieb, E. W. 1976, *Ap. J.*, **203**, 159.
Lillie, C. F., and Witt, A. N. 1973, in *IAU Symposium No. 52, Interstellar Dust and Related Topics*, ed. J. M. Greenberg and H. C. van de Hulst (Dordrecht: Reidel), p. 115.
———. 1976, *Ap. J.*, **208**, 64.
Morton, D. C. 1969, *Ap. J.*, **158**, 629.
O'Dell, C. R., and Hubbard, W. B. 1965, *Ap. J.*, **142**, 591.
Osterbrock, D. E. 1963, *Planet. Space Sci.*, **11**, 621.
Page, T., Carruthers, G. R., and Hill, R. 1978, *S201 Catalog of Far Ultraviolet Objects* (NRL Rept. 8173, 1978 January).
Parker, R. A. R., Gull, T. R., and Kirshner, R. B. 1979, NASA SP-434.
Peimbert, M., and Goldsmith, D. W. 1972, *Astr. Ap.*, **19**, 398.
Pottasch, S. R. 1965, in *Vistas in Astronomy*, Vol. **6**, ed. A. Beer (New York: Pergamon), p. 149.
Schiffer, F. H., and Mathis, J. S. 1974, *Ap. J.*, **194**, 597.
Snow, T. P., and Jenkins, E. B. 1977, *Ap. J. Suppl.*, **33**, 269 (SJ).
Spitzer, L. 1978, *Physical Processes in the Interstellar Medium* (New York: Wiley Interscience).
Thompson, G. I., Nandy, K., Jamar, C., Monfils, A., Houziaux, L., Carnochan, D. J., and Wilson, R. 1978, *Catalogue of Stellar Ultraviolet Fluxes* (London: Science Research Council).
Witt, A. N. 1977, *Pub. A.S.P.*, **89**, 750.
Witt, A. N., and Lillie, C. F. 1978, *Ap. J.*, **222**, 909.

GEORGE R. CARRUTHERS and HARRY M. HECKATHORN: Code 7123, Naval Research Laboratory, Washington, DC 20375

THEODORE R. GULL: Code 683, NASA Goddard Space Flight Center, Greenbelt, MD 20771

PLATE 23

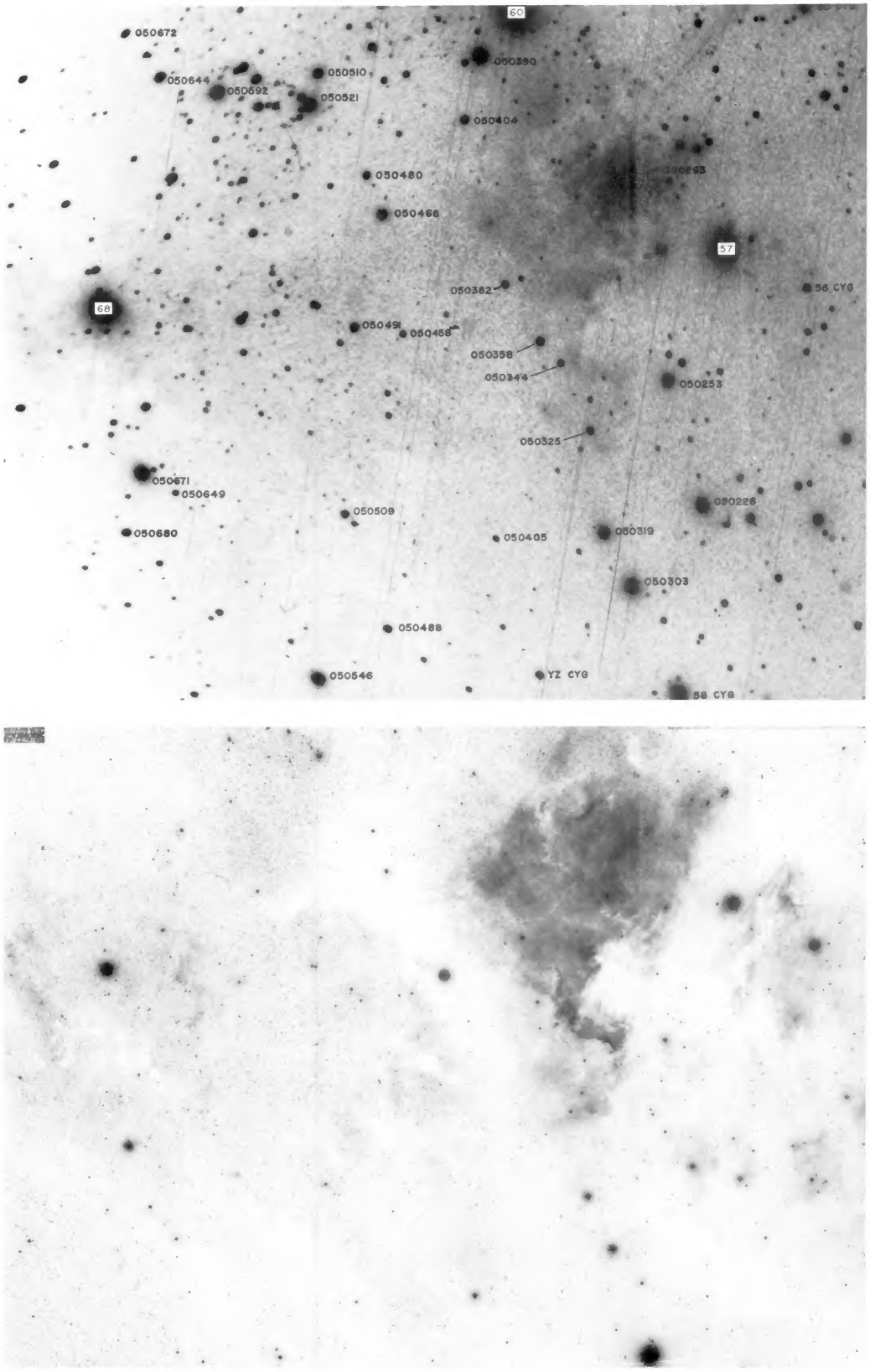

FIG. 1.—A portion of the 50.9 s far-UV (1230–2000 Å) exposure showing the region of the North America Nebula and 68 Cygni, with a ground-based (POSS plate 0-1133) photograph in the blue (3300–5300 Å). SAO and Flamsteed numbers are indicated for the more conspicuous stars of the far-UV image. North is up; west, to the right.

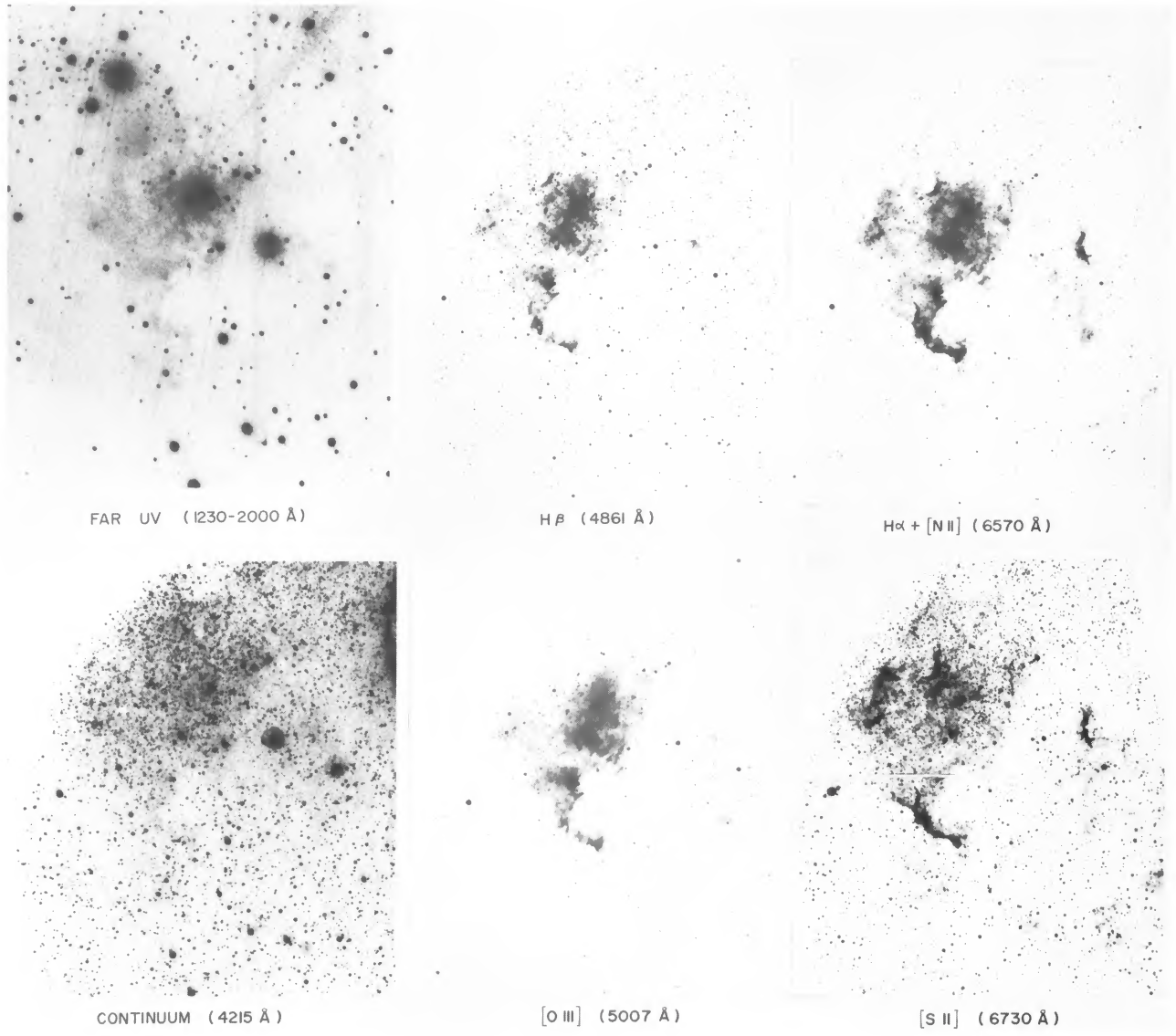

FIG. 2.—The far-UV image of the North America Nebula compared with narrow-band imagery at the wavelengths of visible emission lines and in the continuum. Note that many faint stars contaminate the blue continuum (and to a lesser extent the [S II]) imagery.

CARRUTHERS, HECKATHORN, AND GULL (*see* page 439)

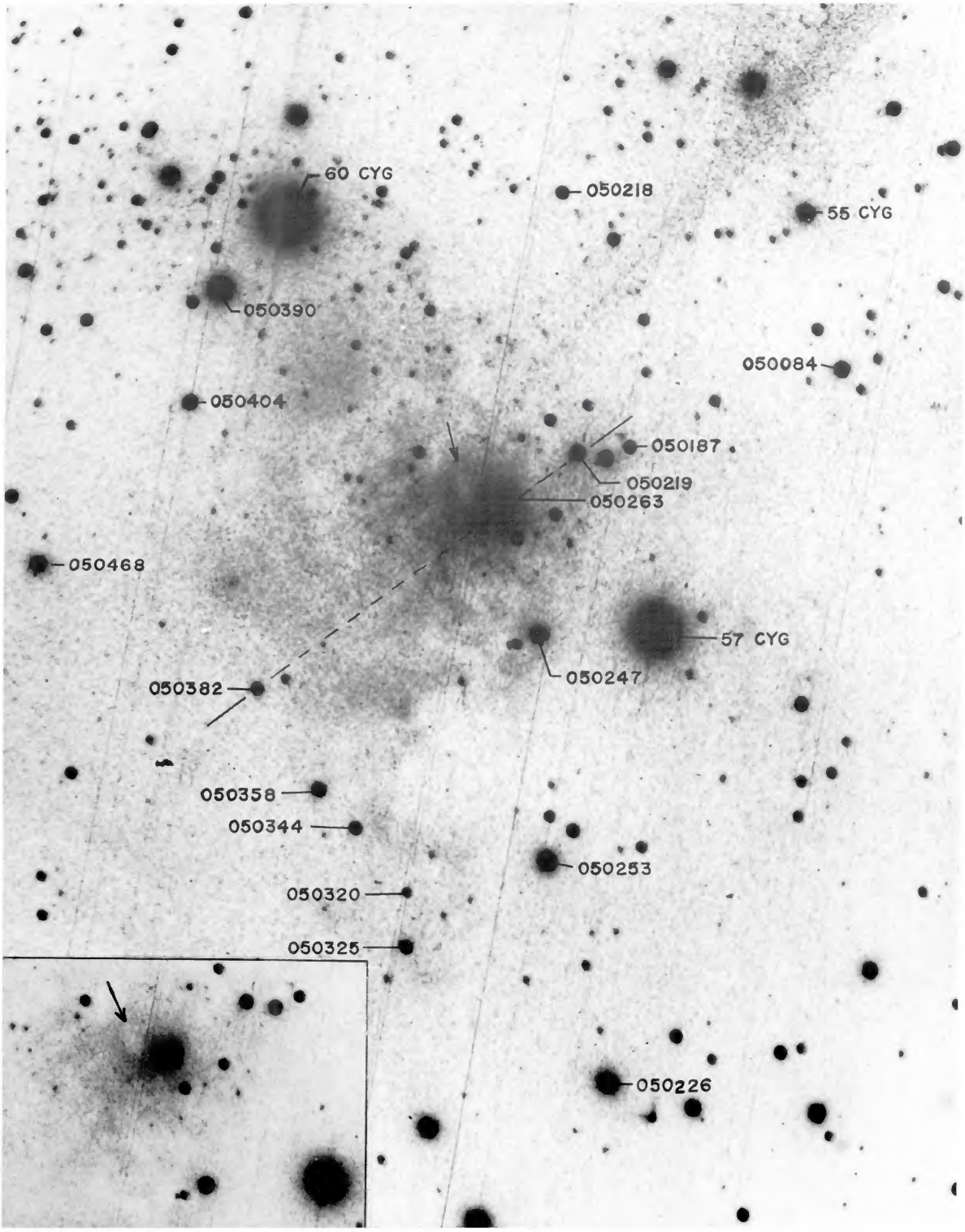

FIG. 3.—An enlargement of the 50.9 s far-UV image of the North America Nebula. The position of a prominent dark cloud NE of HD 199579 (SAO 050263) is indicated by the arrow. The inset shows the immediate vicinity of HD 199579 and is printed to lower contrast to better show details of the nebula in close proximity to the star. The line crossing the nebula between the two indicated SAO stars defines the length and direction of microdensitometer scans used to define the brightness distributions presented in Fig. 9. The width of the area scanned was 1% of the length.